Proceedings of the ASME 2015 34th International Conference on Ocean, Offshore and Arctic Engineering
OMAE2015
May 31-June 5, 2015, St. John's, Newfoundland, Canada

OMAE2015-41312

COMPARISON OF CYCLIC P-Y METHODS FOR OFFSHORE WIND TURBINE MONOPILES SUBJECTED TO EXTREME STORM LOADING

Wystan Carswell
University of Massachusetts Amherst
Amherst, MA, USA

Casey Fontana
University of Massachusetts Amherst
Amherst, MA, USA

Sanjay R. Arwade
University of Massachusetts Amherst
Amherst, MA, USA

Don J. DeGroot
University of Massachusetts Amherst
Amherst, MA, USA

Andrew T. Myers
Northeastern University
Boston, MA, USA

ABSTRACT

Approximately 75% of installed offshore wind turbines (OWTs) are supported by monopiles, a foundation whose design is dominated by lateral loading. Monopiles are typically designed using the *p-y* method which models soil-pile resistance using decoupled, nonlinear elastic Winkler springs. Because cyclic soil behavior is difficult to predict, the cyclic *p-y* method accounts for cyclic soil-pile interaction using a quasi-static analysis with cyclic *p-y* curves representing lower-bound soil resistance. This paper compares the Matlock (1970) and Dunnavant & O'Neill (1989) *p-y* curve methods, and the *p-y* degradation models from Rajashree & Sundaravadivelu (1996) and Dunnavant & O'Neill (1989) for a 6 m diameter monopile in stiff clay subjected to storm loading. Because the Matlock (1970) cyclic *p-y* curves are independent of the number of load cycles, the static *p-y* curves were used in conjunction with the Rajashree & Sundaravadivelu (1996) *p-y* degradation method in order to take number of cycles into account. All of the *p-y* methods were developed for small diameter piles, therefore it should be noted that the extrapolation of these methods for large diameter OWT monopiles may not be physically accurate; however, the Matlock (1970) curves are still the curves predominantly recommended in OWT design guidelines. The National Renewable Energy Laboratory wind turbine analysis program FAST was used to produce mudline design loads representative of extreme storm loading. These design loads were used as the load input to cyclic *p-y* analysis. Deformed pile shapes as a result of the design load are compared for each of the cyclic *p-y* methods as well as pile head displacement and rotation and degradation of soil-pile resistance with increasing number of cycles.

INTRODUCTION

Of the nearly two thousand offshore wind turbines (OWTs) installed globally, approximately 75% are supported by monopile foundations [1]. The lateral load demands on OWT monopiles from wind and wave loading is much larger than the axial demand from self-weight; as such, the calculation of lateral load capacity plays a significant role in design, particularly with respect to the cyclic wind and wave loads. OWT design guidelines (e.g. [2]) recommend the *p-y* curve method for analyzing laterally loaded piles, where soil-pile resistance is modelled by a series of nonlinear springs along the length of the pile per Winkler spring theory.

The recommended *p-y* curves for cyclic load conditions were experimentally determined for small diameter piles assuming a wave-dominated load pattern for offshore platforms [3,4]. The experimental work consisted of displacement-controlled cyclic loading on piles at constant amplitude, with limited information regarding the frequency of the loading or hysteretic behavior of the *p-y* cycles. Moreover, the cyclic loading was applied slowly such that inertial effects were negligible [5]. The resulting cyclic *p-y* curves were used to represent a lower-bound approximation of cyclic soil-pile response, assuming repeated loading of the design wave.

It should be acknowledged that the *p-y* curves were determined for slender piles, unlike the stiff piles (typically 4-7 m in diameter) for OWTs [6]. Despite this concern, the *p-y* method is still the primary recommendation by design guidelines for laterally loaded OWT monopiles.

Cyclic pile-soil behavior plays a role in the assessment of both ultimate limit state (ULS) and serviceability limit state (SLS) for OWT piles, but *p-y* curve methods are recommended primarily for the evaluation of ultimate pile capacity, not SLS [2]. For offshore platform piles, the American Petroleum Institute (API) Recommended Practice SLS as deflections or rotations which would render the structure inadequate for its intended function [7]. For OWT monopiles, the mudline rotation SLS refers to permanent deformations, not transient deformations during cyclic loading. The SLS for OWT monopiles is dictated by the manufacturer and typically on the order of 0.25° of rotation at the mudline after installation; for the ULS, a pile must not exceed some specified pile head displacement, and the designer is cautioned to examine the full force-displacement behavior of the pile to ensure sufficient embedment depth [2].

The purpose of this paper is to compare the OWT monopile head displacement and rotations produced by different cyclic *p-y* curve methods [3,4,8] subjected to extreme storm loading generated for the National Renewable Energy Laboratory (NREL) 5MW Reference Turbine. Because *p-y* methods are meant primarily for the ULS, the SLS is not considered. The assumptions inherent in the *p-y* methods and the applicability of those methods for OWT monopiles are further discussed.

NOMENCLATURE

NREL	National Renewable Energy Laboratory
D&O	Dunnavant & O'Neill (1989)
M-R	Matlock (1970) static *p-y* with Rajashree & Sundaravadivelu (1996) cyclic degradation
OWT	Offshore wind turbine
SLS	Serviceability limit state
ULS	Ultimate limit state
b	Pile diameter
d	Water depth
g	Gravity
p	Soil resistance per unit length
p_u	Ultimate soil resistance per unit length
s_u	Undrained shear strength
u	Pile head displacement
x	Depth below mudline
y	Soil spring displacement
E_p	Young's modulus of the pile
E_s	Young's modulus of the soil
I	Moment of inertia
H	Horizontal mudline force
H_{wave}	Wave height
J	Empirical factor (Matlock 1970)
L	Pile embedment depth
M	Mudline moment
N	Number of cycles
N_{cm}	Cyclic ultimate soil resistance coefficient (D&O)
N_p	Ultimate soil resistance coefficient (D&O)
T	Wave period
U_{hub}	Wind speed
V	Vertical mudline force
ε_c	Strain at 50% of the maximum stress from an undrained compression test
γ'	Effective soil unit weight
λ_N	Degradation factor
θ	Pile head rotation

CYCLIC P-Y MODELS

The two *p-y* methods considered here are from Matlock [3] and Dunnavant & O'Neill ("D&O") [4], experimentally determined using displacement-controlled cycling for slender piles in soft clay and stiff clay, respectively. While the American Petroleum Institute [7] recommends the *p-y* curves developed by Reese, Cox, & Koop (1975) [9] for stiff clays, the clay imbibed water during testing and thus the degradation observed was more severe than in other cases [4]; as such, the D&O *p-y* curves are used here. The equations used to form the Matlock p-y curves can be found in Annex A and D&O p-y curves in Annex B. Examples of both the static and cyclic curves are depicted in Figure 1 given the reference soil properties in Table 1.

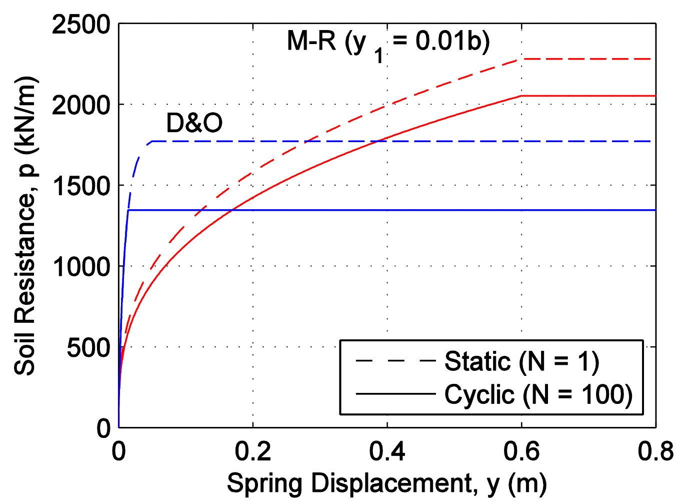

FIGURE 1 STATIC AND CYCLIC P-Y CURVES AT 6 METERS BELOW THE MUDLINE

The Matlock cyclic *p-y* curves represent a quasi-static approximation of minimum soil-pile resistance, assuming an infinite number of cycles independent of number of cycles. The experimental results showed that soil-pile cycling stabilized in less than 100 cycles, with the exception of cyclic deflections exceeding approximately 20% of the pile diameter where progressive deterioration of soil resistance was observed. If this deterioration point is extrapolated for OWT monopiles with diameters between 4.5 and 6 m, this amounts to 0.9-1.2 m cyclic displacements.

For Matlock, the formulation of the static and cyclic *p-y* curves is identical for soil resistance $p \leq 0.72p_u$, where p_u is the ultimate soil resistance. Because of the similarity between the static and cyclic *p-y* curve formulation and because Matlock curves are not a function of the number of cycles, the cyclic *p-y* degradation model by Rajashree & Sundaravadivelu (1996) [8] was used in conjunction with the static Matlock *p-y* curves (defined in Annex A, "M-R").

TABLE 1 REFERENCE SOIL AND PILE PROPERTIES

Property	Value
Undrained Shear Strength, s_u	100 kPa
Strain at 50% of Maximum Stress, ε_c	0.005
Effective Soil Unit Weight, γ'	9.2 kN/m^3
Empirical Factor, J	0.25
Soil Modulus	130 MPa
Pile Diameter, Wall Thickness	6 m, 0.09 m
Pile Embedment Depth	34 m

TABLE 2 NREL 5MW REFERENCE TURBINE PROPERTIES

Property	Value
Hub Height	90 m
Rotor Diameter	126 m
Tower Base Diameter, Wall Thickness	6 m, 0.035 m
Tower Top Diameter, Wall Thickness	3.87 m, 0.025 m
Nacelle & Rotor Mass	350 t
Tower Mass	348 t
Water Depth	20 m
Substructure Diameter, Wall Thickness	6 m, 0.060 m

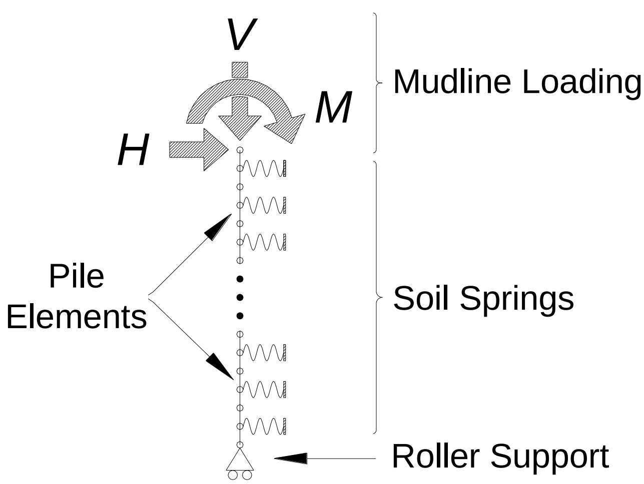

FIGURE 2 P-Y SOIL SPRING MODEL

The cyclic *p-y* degradation model by [8] defines the ultimate soil resistance after a given number of cycles *N* as

$$p_{uN} = (1 - \lambda_N)\, p_u \tag{1}$$

in which p_u is the static ultimate soil resistance, p_{uN} is the degraded ultimate soil resistance, and the degradation factor λ_N can be calculated by

$$\lambda_N = \frac{y_1}{0.2b} \log(N) \leq 1 \tag{2}$$

where y_1 is the static displacement of a given *p-y* spring. In Figure 1, the cyclic curve (defined for N = 100 cycles) shown for this combined M-R method (Matlock static *p-y* curves with Rajashree & Sundaravadivelu degradation method) assumes y_1 = 0.01b.

The D&O *p-y* curve formulation includes a logarithmic degradation of p_u as a function of the depth below soil surface and the number of cycles. For the piles in stiff clay tested, notable degradation from cyclic loading occurred at 1% of the pile diameter. For both the Matlock and D&O experiments, very little degradation in stiffness was seen with increasing number of cycles, which is reflected in the degradation primarily of p_u and not spring stiffness.

The unit stiffness of the soil springs ($\partial p/\partial y$, in units of force per length) for the D&O method is much greater than the Matlock method; however, the ultimate soil resistance of the Matlock curves exceeds D&O.

Both the D&O and Matlock cyclic *p-y* models were formed for cyclic loading conditions which exceeded half of the maximum load of the pile-soil system; as such, caution should be exercised in the interpretation of results for small loads and displacements, as the numerical initial stiffness from the *p-y* curve models are infinite for $\partial p/\partial y|y = 0$.

OFFSHORE WIND TURBINE MODEL

The NREL 5MW Reference Turbine was used in this paper assuming the properties given in Table 2, which was used in conjunction with the NREL aeroelastic program FAST to determine mudline design loads. These mudline loads were then applied to a *p-y* spring model (depicted in Figure 2) informed by the reference soil and pile properties from Table 1.

The *p-y* spring model was nonlinear with respect to soil stiffness and linear with respect to the Euler-Bernoulli beam elements which were used to represent the pile. Nonlinear load-controlled analysis was performed using a second-order Runge-Kutta scheme to determine nonlinear *p-y* spring stiffness. Soil-pile resistance was modeled with soil spring spacing of 2 m (i.e., 17 total springs for a 34 m pile). It is assumed that these soil springs behave symmetrically in tension and compression.

STORM LOADING

NREL's open-source wind turbine software (FAST [10]) was used to model turbine performance under storm loading cases. This program combines aerodynamic, hydrodynamic, structural, and blade element momentum models to simulate OWT response to environmental conditions. No foundation model was included in the FAST analysis. The purpose of this paper is to compare the resultant behavior from different *p-y* models, and thus pure fixity at the mudline was assumed out of simplicity for the generation of mudline loading conditions. FAST takes into account geometric nonlinearity of the tower and blades, but all materials are modeled linearly. The time history analysis was performed using a direct integration scheme with an analysis time step of 0.0125 sec.

In this paper, the NREL 5MW Reference Turbine was sited in 20 m of water off the coast of the state of Massachusetts. The wind loads and wave loads for this site were taken from [11] and conservatively chosen to be co-directional (i.e., no wind-wave misalignment was assumed). Because the site used in this paper for the NREL 5MW Reference Turbine had a water depth of 20 m (versus the 15 m water depth in [11]), the significant wave height which is used as input to FAST for generating irregular waves was scaled linearly by a factor of 1.3 (coming from the ratio of water depths, 20 m/15 m).

Parked design load cases 6.1a, 6.1b, and 6.1c from [12] were analyzed in this paper, excluding cases concerning loss of connection, fatigue limit state, and extreme misalignment. These cases were selected because they represent extreme loading cases during hurricane events when the turbine is parked and feathered. The results for stochastic wind and wave cases (6.1a) were obtained by taking the average maximum horizontal mudline force (H_{max}) and moment (M_{max}) values from six stochastic 1-hour wind and irregular wave time histories, while the results for the steady wind and regular wave cases (6.1b and 6.1c) were obtained by taking the maximum shear and moment for one 10-min simulation.

The peak spectral period (T_p) selected for design load case 6.1a was conservatively selected using the minimum bound offered by [2] for extreme sea states, in which

$$T > 11.1\sqrt{\frac{H_{wave,s}}{g}} \quad \textbf{(3)}$$

where H_s is the significant wave height and g is gravity. For the regular wave design load cases (6.1b and 6.1c), the wave period

$$T > \sqrt{34.5\frac{d}{g}\tanh^{-1}\left(\frac{H_{wave}}{0.78d}\right)} \quad \textbf{(4)}$$

is defined by a depth dependent lower limit derived from wave breaking considerations where d is the water depth.

TABLE 3 ENVIRONMENTAL SITE CONDITIONS AND LOAD SUMMARY FOR MASSACHUSETTS SITE

Design Load Case	U_{hub} (m/s)	H_s (m)	T_p (s)	Yaw Error	H_{max} (MN)	M_{max} (MNm)
6.1a (avg)	47.6	11.3	11.9	-8°	5.93	114.4
				0°	6.32	119
				+8°	5.93	113.5
6.1b	70.1	6.4	5.4	-15°	1.99	74.0
				0°	1.96	65.5
				+15°	2.09	71.9
6.1c	55.1	11.3	8.0	-15°	3.02	75.3
				0°	2.94	74.7
				+15°	2.99	78.4

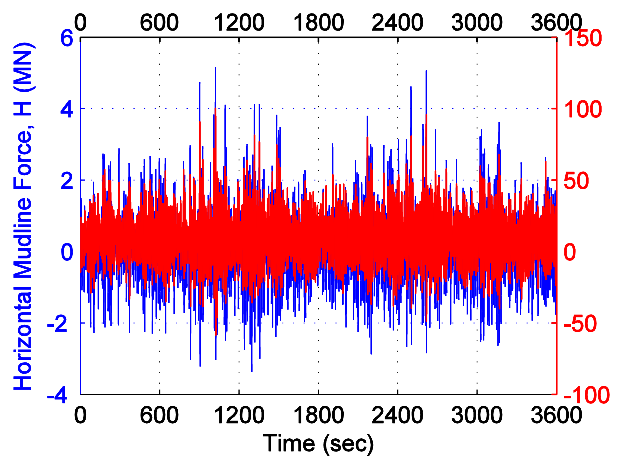

FIGURE 3 EXAMPLE TIME HISTORY OF HORIZONTAL MUDLINE FORCE AND MOMENT FROM DESIGN LOAD CASE 6.1A (0° YAW ERROR)

RESULTS

Table 3 shows that design load case 6.1a with 0° yaw error controls mudline loading. Even though the wind speed is lowest for this case, the design loads are highest due to stochastic loading – the large variation in wind speeds and wave heights yields larger loading maxima as compared to the loading for the constant wind speeds and wave height in 6.1b and 6.1c. For load case 6.1a, inclusion of yaw error decreased H_{max} and M_{max}, but for load cases 6.1b and 6.1c yaw error increased the maximum mudline loads. An example time history from design load case 6.1a is shown in Figure 3.

The mudline values of H_{max} and M_{max} were applied to the top of the *p-y* pile model as well as a gravity load of V = 8.70 MN corresponding to the weight of the rotor-nacelle assembly and self-weight of the tower and substructure. Table 4 contains

TABLE 4 PILE HEAD DISPLACEMENT AND ROTATION RESULTS

			Matlock (1970) [3]				Dunnavant & O'Neill (1989) [4]			
			Static		N = 100[1]		Static		N = 100	
Design Load Case	H_{max} (MN)	M_{max} (MNm)	u_{max} (m)	θ_{max} (°)	u_{max} (m)	θ_{max} (°)	u_{max} (m)	θ_{max} (°)	u_{max} (m)	θ_{max} (°)
6.1a (average)	5.93	114.4	0.038	0.152	0.041	0.158	0.012	0.079	0.014	0.086
	6.32	119.0	0.043	0.167	0.047	0.176	0.013	0.083	0.015	0.092
	5.93	113.5	0.038	0.150	0.040	0.157	0.012	0.078	0.013	0.086
6.1b	1.99	74.0	0.009	0.054	0.009	0.055	0.005	0.040	0.005	0.042
	1.96	65.5	0.008	0.048	0.008	0.048	0.004	0.036	0.005	0.037
	2.09	71.9	0.009	0.054	0.009	0.054	0.005	0.039	0.005	0.041
6.1c	3.02	75.3	0.012	0.065	0.012	0.065	0.006	0.044	0.006	0.046
	2.94	74.7	0.012	0.064	0.012	0.064	0.006	0.044	0.006	0.046
	2.99	78.4	0.013	0.067	0.013	0.068	0.006	0.046	0.007	0.048

[1]Combined with degradation model by Rajashree & Sundaravadivelu (1996) [8].

the peak displacements and rotations for all load cases, comparing the response of the *p-y* spring models from Matlock, M-R, and D&O for both static and cyclic cases (assuming N = 100). The force-displacement curves associated with the pile head displacements in Table 4 are shown in Figure 4, with dotted lines and open markers indicating static response and solid lines with X markers indicating cyclic response.

Table 4 and the force-displacement paths in Figure 4 show that very little degradation occurs for even the controlling load case for the given soil conditions and pile design, with the static and cyclic force-displacement paths nearly indistinguishable from one another for the Matlock and M-R models. This is likely due to the fact that the displacements (and therefore strains within the soil) are very small for a monopile in stiff

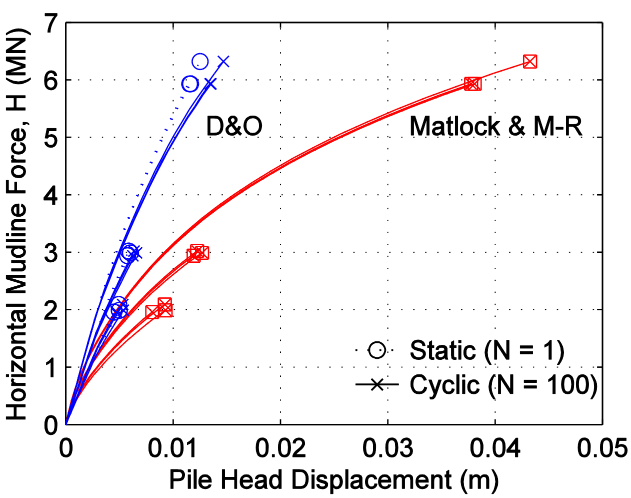

FIGURE 4 COMPARISON OF FORCE-DISPLACEMENT CURVES FOR ALL DESIGN LOAD CASES.

clay. If monopile with the same embedment depth were in a medium clay with s_u = 50 kPa for instance, the M-R pile head displacement would be approximately five times larger and the D&O pile head displacement approximately 2.5 times larger. In these cases, the embedment depth of the pile would likely be increased to mitigate pile head displacement.

Figure 4 also shows the fairly linear behavior of the D&O *p-y* spring model at these load levels and highly nonlinear behavior of the Matlock *p-y* spring model. For the most extreme case, the M-R *p-y* model predicts over three times the pile head displacement as the D&O model.

In order to further investigate the differences between these models, the deformation of the pile-soil system for both models were compared (Figure 5). It is immediately clear that the M-R *p-y* spring model is behaving quite flexibly, with a significant amount of pile toe-kick; consequently, the embedment depth would need to be increased in order to provide sufficient fixity at the pile toe to improve pile design. The D&O model behaves more rigidly overall. The M-R *p-y* spring model is more conservative than D&O, but in the absence of full-scale monopile data it cannot be determined whether the model is conservative or questionably applicable due to flexible pile assumptions and the fact that the original experiments performed by [3] were in soft clay.

The rigid vs. flexible pile behavior is further underscored in Figure 6, where the mobilization of soil spring resistance was assessed for the controlling design load case was plotted along the depth of the pile. Despite the higher magnitude displacements from the Matlock *p-y* model, the D&O *p-y* springs are mobilized to approximately the same degree. It must be noted once again that the ultimate soil resistance p_u is lower for D&O than Matlock, so soil spring mobilization represents the distribution of force along the length of the pile and the relationship between the stiffness of the pile and the stiffness of the soil. The inflection point in the Matlock *p-y* spring model is clearly visible at approximately 22 m below the mudline, whereas the mobilization diagram of the D&O *p-y* model smoothly transitions from the base to the top. The D&O method also has nearly 10% more mobilization in the top 5 m of the soil, indicating that soil springs in these areas are in higher demand than for M-R.

It is also interesting to note that the M-R model does not exceed p/p_u = 0.72, which means that soil-pile behavior is expected to act identically for static and cyclic conditions if the strict definition of the *p-y* curves is adhered to (see Annex A).

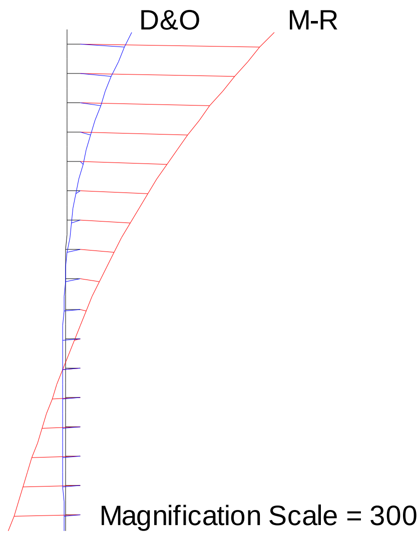

FIGURE 5 PILE DEFORMATIONS FOR CONTROLLING DESIGN LOAD CASE WITH DEPTH CONSIDERING 100 CYCLES OF LOADING

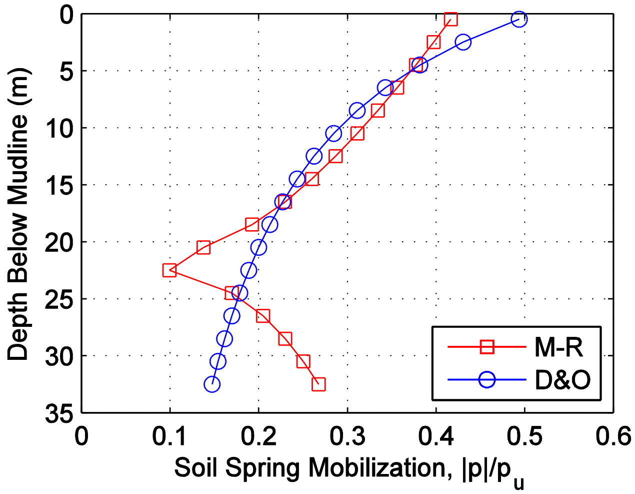

FIGURE 6 SOIL SPRING MOBILIZATION FOR CONTROLLING DESIGN LOAD CASE WITH DEPTH FOR 100 CYCLES OF LOADING

Lastly, it should be noted that the degradation methods used for the two *p-y* models differ significantly; shows ratio of pile head displacement after one cycle (u_1) to the pile head displacement after N number of cycles (u_N). It is immediately clear in Figure 7 that the D&O soil-pile system degrades much faster than the M-R system. In the case of the M-R soil-pile system, degradation plateaus around N = 500 at approximately u_1/u_N = 1.08, whereas the D&O degradation continues to increase beyond u_1/u_N = 1.2 and does not clearly level off within the 1000 cycles considered here.

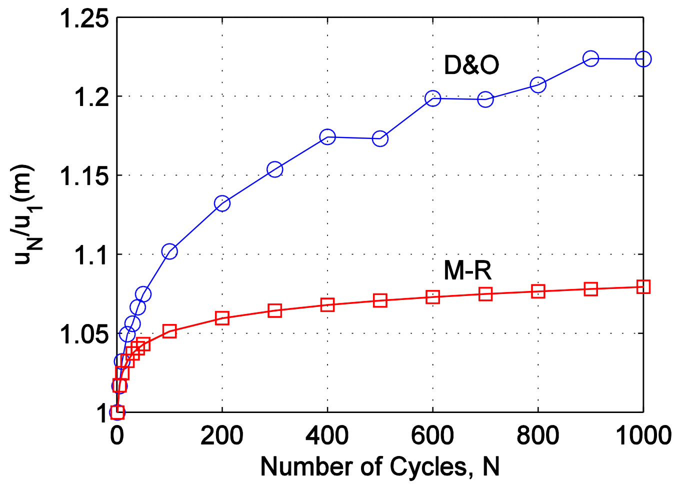

FIGURE 7 INCREASE IN PILE HEAD DISPLACEMENT WITH NUMBER OF CYCLES FOR CONTROLLING DESIGN LOAD CASE

The D&O degradation is also not as smooth as the M-R degradation, indicating that some of the soil springs are fully mobilized and have begun to behave plastically, causing a redistribution of forces amongst the remaining soil springs. This redistribution is not observed in the M-R system due to the higher ultimate soil resistance of the Matlock *p-y* curves.

Given that the controlling design load case is representative of a 50-year storm, it is highly unlikely that an OWT monopile would experience even as many as 100 cycles during a design lifetime; however, it is useful to examine degradation behavior if only to ensure that the *p-y* pile design remains adequate for a great many cycles.

CONCLUSIONS

This paper compared the cyclic *p-y* methods from Matlock (1970) [3] and Dunnavant & O'Neill (1989, "D&O") [4] in application to OWT monopile foundations in stiff clay subjected to extreme storm loading. Because the static and cyclic Matlock *p-y* curves are identical for soil spring mobilization $p/p_u \leq 0.72$ and are independent of the number of load cycles, the *p-y* spring degradation method developed by Rajashree & Sundaravadivelu (1996) [8] was used in conjunction with the static Matlock *p-y* curves ("M-R"). The primary conclusions of this paper are as follows:

- While the Matlock *p-y* curves are recommended by design guidelines for piles in clay (e.g. [2]), the soil-pile system demonstrates very flexible behavior which may or may not be congruent with the rigid behavior of an OWT monopile (which traditionally range from approximately 4-6 m).
- The D&O method demonstrated much more rigid behavior than M-R, with pile head displacements from the controlling design load case as much as five times smaller.
- Pile head displacement degraded at a much faster rate for D&O and did not plateau within the 1000 cycles considered, whereas the degradation plateaued for the M-R case after approximately 500 cycles.

It is unclear how conservative the M-R *p-y* method is when compared the D&O *p-y* method in the absence of experimental data for full-scale OWT monopile foundations. Additionally, it should be noted that all the results presented in this paper assumed the same monopile design; further work on this topic could include a comparison of monopile design using the two different *p-y* methods presented.

ACKNOWLEDGMENTS

The research was supported by the grants CMMI-1234560, CMMI-1234656, the Massachusetts Clean Energy Center and the NSF-sponsored IGERT: Offshore Wind Energy Engineering, Environmental Science, and Policy (Grant Number 1068864).

REFERENCES

[1] Hamilton, B., Battenberg, L., Bielecki, M., Bloch, C., Decker, T., Frantzis, L., Paidipati, J., Wickless, A., and Zhao, F., 2013, Offshore Wind Market and Economic Analysis: Annual Market Assessment, Navigant Consulting, Inc., Burlington, MA.

[2] DNV, 2013, DNV-OS-J101 Design of Offshore Wind Turbine Structures, Det Norske Veritas AS.

[3] Matlock, H., 1970, “Correlations for design of laterally loaded piles in soft clay,” Offshore Technology Conference, Dallas, TX.

[4] Dunnavant, T. W., and O’Neill, M. W., 1989, “Experimental p-y Model for Submerged, Stiff Clay,” J. Geotech. Eng., **115**, pp. 95–114.

[5] Kramer, S., 1988, Development of Py Curves for Analysis of Laterally Loaded Piles in Western Washington.

[6] Klinkvort, R. T., Leth, C. T., and Hededal, O., 2010, “Centrifuge modelling of a laterally cyclic loaded pile,” International Conference on Physical Modelling in Geotechnics, Taylor & Francis Group, Zurich, Switzerland, pp. 959–964.

[7] American Petroleum Institute, 2005, “API RP-2A.”

[8] Rajashree, S. S., and Sundaravadivelu, R., 1996, “Degradation model for one-way cyclic lateral load on piles in soft clay,” Comput. Geotech., **19**(4), pp. 289–300.

[9] Reese, L., Cox, W., and Koop, F., 1975, “Field Testing and Analysis of Laterally Loaded Piles in Stiff Clay,” Offshore Technol. Conf.

[10] Jonkman, J., and Buhl, M. J., 2005, FAST User’s Guide, National Renewable Energy Laboratory, Golden, CO.

[11] MMI Engineering, 2009, “Comparative Study of OWTG Standards Prepared for JIP Sponsorship MMI Engineering , Inc .”

[12] IEC 61400-3, 2009, Design Requirements for Offshore Wind Turbines, Brussels.

[13] O’Neill, M., Reese, L., and Cox, W., 1990, “Soil behavior for piles under lateral loading,” Offshore Technol. Conf.

ANNEX A

MATLOCK (1970) P-Y CURVE EQUATIONS

The equations for *p-y* curves developed by Matlock (1970) [3] are given below, where p is the nonlinear soil resistance of a soil spring at a depth x below the mudline which varies as a function of the soil spring displacement y.

The static *p-y* curves (which were used in conjunction with the degradation method proposed by Rajashree & Sundaravadivelu (1996) [8]) are defined by

$$p = \begin{cases} 0.5 p_u \left(\dfrac{y}{y_c} \right)^{1/3} & \text{for } y \le 8 y_c \\ p_u & \text{for } y > 8 y_c \end{cases} \tag{5}$$

where

$$y_c = 2.5 \varepsilon_c b \tag{6}$$

and

$$p_u = \begin{cases} (3 s_u + \gamma' x) b + J s_u x \le 9 s_u b & \text{for } 0 < X \le X_R \\ 9 s_u & \text{for } X > X_R \end{cases} \tag{7}$$

in which ε_c is the strain at 50% of the maximum stress from an undrained compression test, b is the pile diameter, s_u is the undrained shear strength, γ' is the submerged unit weight, and J is an empirically determined coefficient which ranges from 0.25 for overconsolidated clays to 0.5 for soft normally consolidated clays. The transition depth X_R is the point below the mudline at which the ultimate soil resistance p_u is controlled by $9 s_u b$.

The response of the soil-pile system under cyclic loading is defined different for soil springs above and below the transition depth, X_R. For cyclic *p-y* curves where $x < X_R$,

$$p = \begin{cases} 0.5 p_u \left(\dfrac{y}{y_c} \right)^{1/3} & \text{for } y \le 3 y_c \\ 0.72 p_u & \text{for } y > 3 y_c \end{cases} \tag{8}$$

whereas cyclic *p-y* curves for $x \le X_R$ are defined by

$$p = \begin{cases} \dfrac{p_u}{2} \left(\dfrac{y}{y_c} \right)^{1/3} & \text{for } y \le 3 y_c \\ 0.72 \mathrm{p_u} \left(1 - \left(1 - \dfrac{X}{X_R} \right) \dfrac{y - 3 y_c}{12 y_c} \right) & \text{for } 3 y_c < y \le 15 y_c \\ 0.72 \mathrm{p_u} \dfrac{\mathrm{X}}{\mathrm{X_R}} & \text{for } y > 15 y_c \end{cases} \tag{9}$$

which accounts for the degradation of soil resistance under cyclic loading.

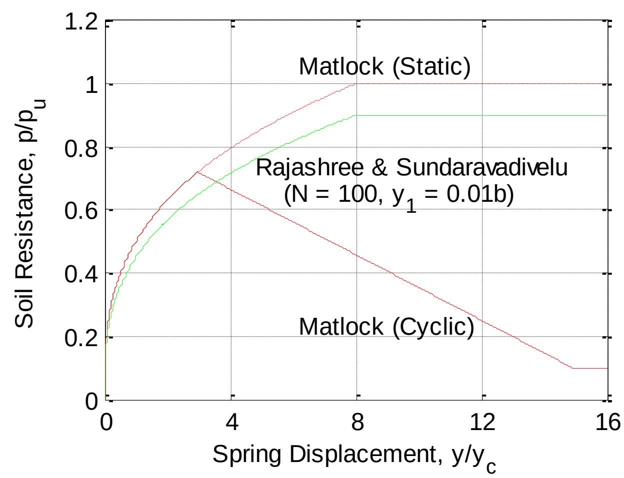

FIGURE 8 MATLOCK (1970) [3] **P-Y MODELS WITH RAJASHREE & SUNDARAVADIVELU (1996)** [8]

ANNEX B

DUNNAVANT & O'NEILL (1989) P-Y CURVE EQUATIONS

The equations for *p-y* curves developed by Dunnavant & O'Neill (1989) [4] are given below, where *p* is the nonlinear soil resistance of a soil spring at a depth *x* below the mudline which varies as a function of the soil spring displacement *y*. These *p-y* curves are a hyperbolic tangent function described by

$$p = 1.02\,p_u \tanh\left[0.537\left(\frac{y}{y_c}\right)^{0.70}\right] \text{for } y \le 8y_c \tag{10}$$

where y_c is defined by

$$y_c = 0.0063\varepsilon_c b K_R^{-0.875} \tag{11}$$

in which

$$K_R = \left(\frac{EI}{E_s L^4}\right) \tag{12}$$

where *EI* is the bending stiffness of the pile, E_s is the soil modulus, and *L* is the length of the pile, limited numerically to the critical pile length

$$L_{crit} = 3b\left(\frac{EI}{E_s b}\right)^{0.286}. \tag{13}$$

In this paper, E_s was approximated using the upper bound suggested value of $200s_u$ from [3], which also agrees approximately with the soil properties in the typical set of conditions given in [13].

Under cyclic loading, this method degrades the ultimate resistance p_u according to the number of load cycles *N*, such that

$$p_u = N_{cm} s_u b \tag{14}$$

and

$$N_{cm} = N_p\left(1-\left(0.45-0.18x\right)\log N\right) \le 1-0.12\log N, \tag{15}$$

wherein

$$N_p = \left(2+\frac{\sigma'_v}{s_{ua}}+0.4\frac{x}{b} \le 9\right) \tag{16}$$

where σ'_v is the vertical effective stress and s_{ua} is the average undrained strength of the soil to depth *x*.